Robotica (2008) volume 26, pp. 55–62. © 2007 Cambridge University Press
doi:10.1017/S026357470700358X Printed in the United Kingdom

Development of a new buffing robot manipulator for shoes

Hyeung-Sik Choi*, Gyu-Deuk Hwang and Sam-Sang You

Division of Mechanicl and Information Engineering, Underwater Vehicle Research Center, Korea Maritime University, Dongsam-Dong, Yeongdo-Ku, Pusan, Korea.

(Received in Final Form: May 16, 2007. First published online: August 28, 2007)

SUMMARY

This paper presents analysis and experimental verifications of a new robot manipulator with five degrees of freedom developed for the buffing operation of shoes. First, the forward and inverse kinematics are analyzed. Next, an analytic closed-form solution is rigorously derived for the joint angles corresponding to the position and orientation of the end-effector in Cartesian coordinates. A control system, including input/output interfaces and the related electronic system, is designed for the control of the mechanical structure of the buffing robot. Then, peripheral systems integrated with the conveyer, transfer device, and fixture device are designed for the sequential buffing process of shoes. Also, a graphic user interface (GUI) program including the forward/inverse kinematics, control algorithm, and communication program to interact the robot with the peripheral systems is developed by using visual C++ language. A new flexible toolholder (FTH) is proposed to compensate for the excessive applied force between deburring tools and shoes. Finally, the test results are provided to demonstrate the effectiveness of the proposed scheme.

KEYWORDS: Robot manipulator; Buffing; Shoe uppers; Kinematics; Control system; Flexible toolholder.

1. Introduction

In general, shoe processing tasks are tedious and relatively complicated such that several machines have been applied to tasks in footwear production factories. In one of the processing tasks, the leather uppers of the shoe exterior are glued to the outsole. Since the leather uppers of the shoe exterior are treated with various dyes or they have slippery surfaces, it is not easy to maintain a high level of adhesion between the leather uppers and the outsole of the shoes. Hence, the side of the uppers covering the sole should be mechanically buffed to enhance the adhesive power. This task is tedious and hazardous to human health because of the amount of dirt involved, and demands higher labor costs as well. In this sense, developing automatic buffing machines for processing of the shoe uppers has been actively pursued in the shoemaking industry.

Considerable attention has been paid to the development and applications of industrial robots in shoe manufacturing for tasks such as the buffing task of shoes. Many commercially available industrial robots have been used in manufacturing and assembly tasks in several shoe companies. The early work done by Tectors Company in England was noticed by many shoe manufacturers. In 1989, this company introduced the PUMA 700 commercial robot for buffing the uppers of shoes. Recently, the ABB Robot Company in Sweden has conducted similar tasks for shoe buffing.

In addition, the robot system applied to shoe manufacturing was investigated by Spencer.[1] It has been recognized that the shoe industry is turning more and more toward the robot-based automation system capable of autonomous and repetitive operations. Furthermore, several other shoe companies such as ACTIS (France), DESMA (Germany), and Intelligent Machines (USA) have used industrial robots for shoe manufacturing.[2]

Research on various types of robots applied to shoe processing tasks such as outsole buffing has been conducted for real applications. However, most of these robots are applied to formalized shoes, and the existing 6-axis industrial robots have been utilized for the buffing tasks. It has been observed that industrial robots are often too expensive and not appropriate for the buffing operation of irregular shoes such as public sneakers. Furthermore, to apply industrial robots to the buffing operation of shoes, a user-oriented program is required to achieve easy interface between operators and robots. For this reason, practical dedicated robots with user-oriented programs are required for buffing the outsole of shoes including public sneakers.

The purpose of this study is to develop a new 5-degree-of-freedom (DOF) buffing-oriented robot capable of performing buffing operations for general shoes. The forward and inverse kinematics of the developed robot are completely analyzed, and the peripheral devices and control system for sequential process tasks are designed. A trajectory control program for the robot is developed to automatically follow a desired buffing task line, and a communication system between the robot and the peripheral system is developed as well. Furthermore, the program for a graphic user interface (GUI) based on the visual C++ language is designed for the buffing robot, so that the user can conveniently manipulate and teach the robot via the operating screen. In addition, a new structure of the flexible toolholder (FTH) is proposed and analyzed to compensate the interacting forces between the buffing tools and shoes.

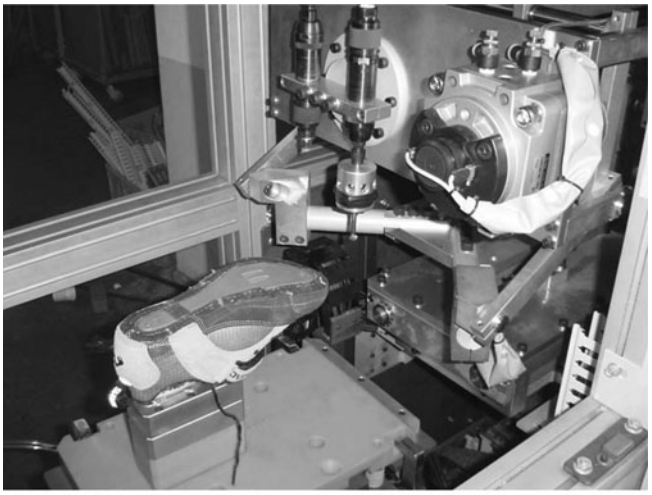
2. Kinematics of the Robot

2.1. *Forward kinematics analysis of robot*

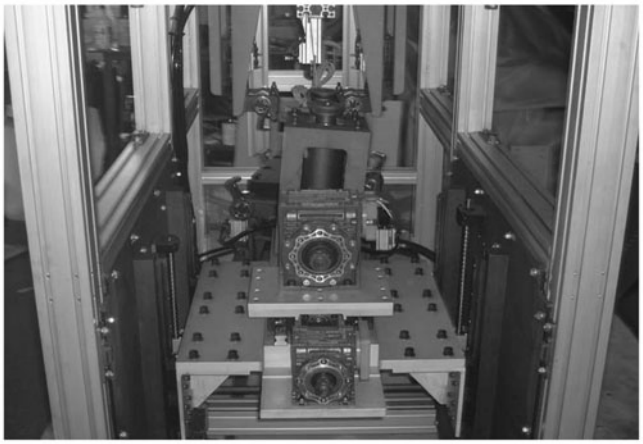
In this study, a new robot system is proposed for the buffing tasks of shoe uppers as shown in Fig. 1(a) and (b),

* Corresponding author. E-mail: hchoi@hhu.ac.kr

https://doi.org/10.1017/S026357470700358X Published online by Cambridge University Press



(a)



(b)

Fig. 1. (a) Front side of the developed robot. (b) Rear side of the developed robot.

where the system structure consists of five driving axes. For a broad class of applications in the workspace, the robot, in principle, requires six axes to exactly describe the positions and orientations of the end-effector in space. Since the configuration of the shoe has similar set-form shapes such that the buffing trajectories are almost uniform, we propose a new robot featuring reduced number of axes exclusively for the buffing tasks for shoes.

The developed robot has five axes relative to the fixed base frame; four axes for successive chain mechanisms, and one for an independent structure like a positioner. The buffing robot featuring revolute joints and four-bar linkages is schematically shown in Fig. 2, excluding the lower two axes for linear motions. Figure 1 shows a control system for the robot, in which the buffing tool attached to the end-effector is intended to follow the trajectory on the workspace. To accomplish this, the points of the trajectory expressed in the coordinates of the workspace should be transformed to the corresponding joint angles with respect to the base frame. These coordinate transformations can be accomplished by using forward and inverse kinematics relations.[3,4]

As shown in Fig. 3, the prismatic joints in the buffing robot are involved in the frames 0 and 1 through ballscrews,

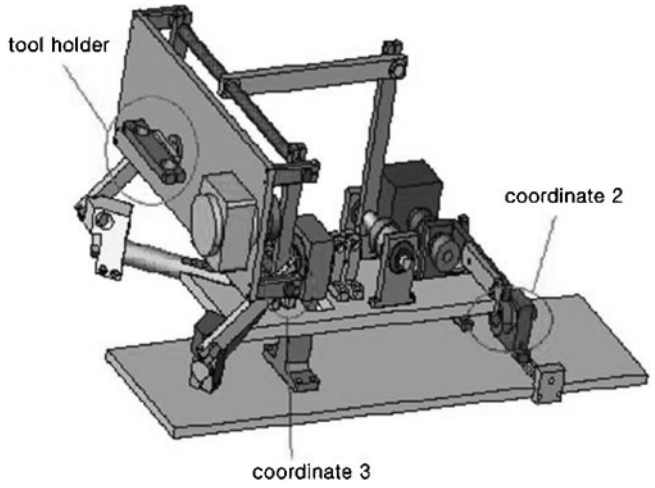


Fig. 2. Schematic diagram of the developed robot.

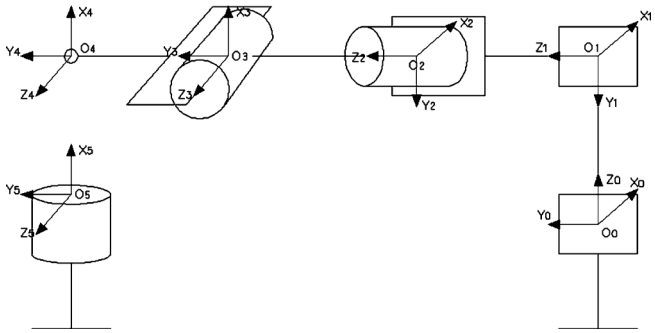


Fig. 3. D-H convention used in the robot manipulator.

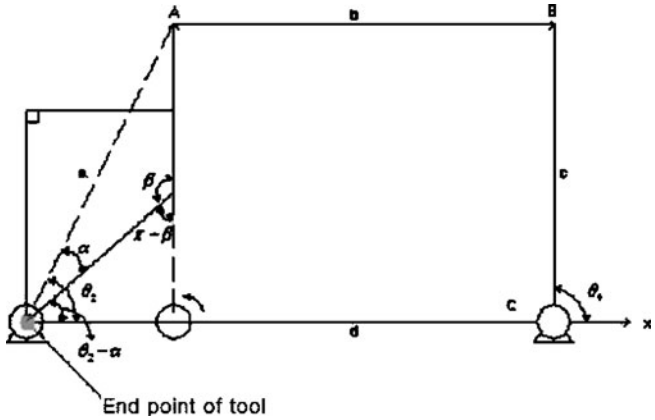


Fig. 4. The relationship between four-bar linkage and joint angle.

and the frames 2, 3, and 5 have all revolute joints. Finally, the fourth wrist joint shown in Fig. 4 is intended to provide significant torques because it uses four-bar linkages. Here, a motor is installed at the end of the ballscrew to determine the joint angle θ_4, and depending on the rotation of the motor, the angle $\theta_2 - \alpha$ is calculated by the Freudenstein equation.[5] Furthermore, a motor is installed at the four-bar linkages **c** and then depending on the corresponding rotation of the motor, it can rotate the buffing tool attached to the end-effector in turn.

https://doi.org/10.1017/S026357470700358X Published online by Cambridge University Press

Table I. Link parameters by D-H notation for the robot.

Link	a_i	α_i	d_i	θ_i
1	0	−90	d_1^a	0
2	0	0	d_2^a	0
3	0	90	d_3	θ_3^a
4	0	0	d_4	θ_4^a

[a] Variable.

Basically, the buffing robot was constructed to have a connected mechanism with the peripheral system transporting the last covered by the shoe within the workspace through a conveyor. The last, placed on the conveyor, is transported to an arbitrary place in the workspace of the robot for buffing tasks. If the buffing points of the last are given in the Cartesian coordinates, then the displacement of each joint angle can be determined by using the forward and inverse kinematics equations with respect to the tool frame.

Figure 3 shows the D-H convention[6] of the robot, taking the coordinates from 0 to 4 and excluding independent frame 5. The corresponding robot parameters are described in Table I.

Now, the homogeneous transformation T_0^4 matrix from the coordinate 0 into those of frame 4 is calculated based on previously defined link parameters, and is thus given by

$$T_0^4 = \begin{pmatrix} \cos\theta_3^*\cos\theta_4^* & -\cos\theta_3^*\sin\theta_4^* & \sin\theta_3^* & d_4\sin\theta_3^* \\ \sin\theta_4^* & \cos\theta_4^* & 0 & d_3+d_2^* \\ -\sin\theta_3^*\cos\theta_4^* & \sin\theta_3^*\sin\theta_4^* & \cos\theta_3^* d_4 & \cos\theta_3^* d_1^* \\ 0 & 0 & 0 & 1 \end{pmatrix}. \tag{1}$$

The transformation matrix Eq. (1) clearly offers information on the orientation and position matrix for coordinates 4 through 0.

2.2. *Inverse kinematics analysis of robot*

Each joint angle information for coordinates from 0 to 4 in the workspace is required to determine the tool frame attached at the end-effector. In contrast, once the coordinate points for the buffing works in the workspace are given, the joint angles can be determined by solving inverse kinematics for coordinates 0 through 4 and the linear distance for coordinate frame 5. Then, the homogeneous transformation matrix H_0^5 used to transform the coordinates from 0 to 5 can be written as

$$H_0^5 = \begin{pmatrix} \cos\theta_5^* & -\sin\theta_5^* & 0 & d_x \\ \sin\theta_5^* & \cos\theta_5^* & 0 & d_y \\ 0 & 0 & 1 & d_z \\ 0 & 0 & 0 & 1 \end{pmatrix} \tag{2}$$

where d_x, d_y, and d_z, respectively, represent the predefined translational positions of coordinate 5 (with origin O_5) relative to the corresponding directions of the reference frame O_0–$x_0y_0z_0$. As shown in Fig. 5, the buffing points used by the robot to follow the trajectory are those based on coordinate frame 5.

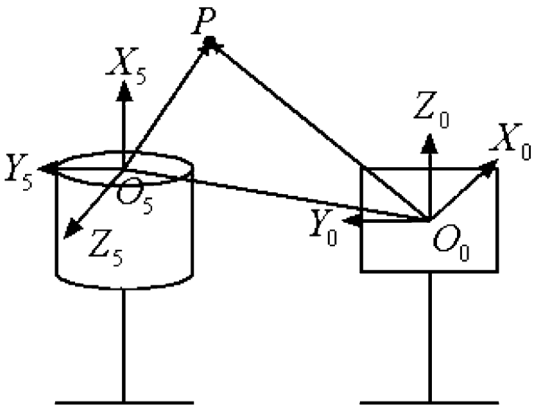


Fig. 5. Relationship between coordinate axis 5 and coordinate axis 0.

From the earlier discussion, we conclude $P_0 = H_0^5 P_5$. Thus, this is expressed by

$$P_0 = \begin{pmatrix} \cos\theta_5^* & -\sin\theta_5^* & 0 & d_x \\ \sin\theta_5^* & \cos\theta_5^* & 0 & d_y \\ 0 & 0 & 1 & d_z \\ 0 & 0 & 0 & 1 \end{pmatrix} \begin{pmatrix} P_x \\ P_y \\ P_z \\ 1 \end{pmatrix} = \begin{pmatrix} P_x\cos\theta_5^* - P_y\sin\theta_5^* + d_z \\ P_x\sin\theta_5^* + P_y\cos\theta_5^* + d_y \\ P_z + d_z \\ 1 \end{pmatrix}. \tag{3}$$

In addition, P_o represents the points of the buffing trajectory in the reference frame and are the corresponding positions of the 4th column of T_0^4 in Eq. (1) determined by forward kinematics. Accordingly, we can obtain the following relations

$$P_x\cos\theta_5^* - P_y\sin\theta_5^* + d_z = d_4\sin\theta_3^* \tag{4}$$

$$P_x\sin\theta_5^* + P_y\cos\theta_5^* + d_y = d_3 + d_2^* \tag{5}$$

$$P_z + d_z = d_4\cos\theta_3^* + d_1^*. \tag{6}$$

Equations 4–6 represent the relationship between positions and joint angles of the buffing points with respect to the reference frame.

To coordinate the buffing tool of the robot, the position and orientation of the buffing tool can be decided by using the derived model. However, the corresponding joint angles are calculated by the normal vector of the buffing points. To determine the accurate orientation of the tool for the given tasks, three tool angles are generally required. Since the shapes of shoes are generally regular, requiring one constraint for the orientation of the tool, two tool angles are simply enough to determine the orientation of the tool. Hence, the three rotations about the axes x, y, z (referring to the roll, pitch, and yaw angles) with respect to the reference frame

https://doi.org/10.1017/S026357470700358X Published online by Cambridge University Press

can be expressed in matrix form as

$$R_0^4 = R_{Z,\phi} R_{Y,\theta} R_{X,\psi}$$
$$= \begin{pmatrix} C\phi C\theta & -S\phi C\psi + C\phi S\theta S\psi & S\phi S\psi + C\phi S\theta C\psi \\ S\phi C\theta & C\phi S\psi + S\phi S\theta S\psi & -C\phi S\psi + S\phi S\theta C\psi \\ -S\phi & C\theta S\psi & C\theta C\psi \end{pmatrix}$$
$$= \begin{pmatrix} r_{11} & r_{12} & r_{11} \\ r_{21} & r_{22} & r_{23} \\ r_{31} & r_{32} & r_{33} \end{pmatrix} \quad (7)$$

where r_{ij} represents an element of the rotation matrix. Note that Eq. (7) describes a user-defined matrix of the tool angles for the tasks in the reference frame. Since only two tool angles are used in this study, the rotation matrix part in Eq. (1) satisfies both Eq. (4) and the rotation matrix in Eq. (7). In this sense, we obtain $r_{23} = 0$ by comparing these rotation matrices, or the constraints

$$-C\phi S\psi + S\phi S\theta C\psi = 0. \quad (8)$$

When setting up the tool angles, the condition for Eq. (9) is required. Also, comparison of Eq. (1) with Eq. (7) leads to $\frac{r_{21}}{r_{22}} = \tan\theta_4^*$. It follows that

$$\theta_4^* = A\tan(r_{21}, r_{22}). \quad (9)$$

Similarly, we obtain the analytic solution for θ_3^* as

$$\theta_3^* = A\tan(r_{13}, r_{33}). \quad (10)$$

From Eq. (6),

$$d_1^* = p_z - d_z - d_4\cos\theta_3^*. \quad (11)$$

Squaring d_z and d_y from both sides of Eqs. (4) and (5) and rearranging them yields

$$d_2^* = d_y - d_3 \pm \sqrt{P_x^2 + P_y^2 - (d_4\sin\theta_3^* - d_z)^2}. \quad (12)$$

Finally, by squaring p_x and p_y in Eqs. (4) and (5), a solution for θ_5^* is readily shown to be

$$\theta_5^* = A\cos\left\{((d_3 + d_2^* - d_y)P_y + (d_4\sin\theta_3^* - d_z)P_x)\Big/\left(P_x^2 + P_y^2\right)\right\}. \quad (13)$$

Consequently, once the tool angles satisfying constraints in Eq. (8) are given, the robot joint angles can be determined in real-time by using the analytic solutions from Eqs. (9)–(13)

3. Overall Structure of Buffing Robot System

3.1. Control system with peripheral systems

The robot system presented in this paper consists of the robot for buffing operations and the peripheral systems integrated with the conveyer, transfer device, fixing jig for the last, and communication units with the developed GUI program for easy operations. The buffing operations are performed in a sequential process programmed by the operator by using the developed GUI. For example, the shoes on the last are transferred to a predefined position in the workspace of the robot by means of the transfer device from the conveyor. According to the signal from the position sensor notifying the arrival of the last, the shoe last is fixed by the jig, and then the robot carries out the buffing operation.

The buffing robot with five axes is capable of loading various buffing tools. Two base joints with axes x_0 and x_1 of the robot are operated for linear motions and the other three joints are operated for rotational motions. Specifically, the arm joint with axis x_2 at the end of the robot adopts the four-bar-link mechanism.

For the motor control at each joint of the robot, the multimotion controller (MMC) made by the Samsung Corp. was implemented. The programmable logic controller (PLC) (model: Master-K), a product of the Mitsubishi Corp., was adopted as the sequential controller of the peripheral systems, and it was sequentially programmed to control the peripheral systems including the buffing robot. The control system with the motor driver and input/output (I/O) interface system including the PLC and peripheral systems are illustrated in Figs. 6 and 7, respectively.

3.2. Code for the control system

We have composed a source code for the control and operation of the robot system by using visual C/C++



Fig. 6. Motor driver system.

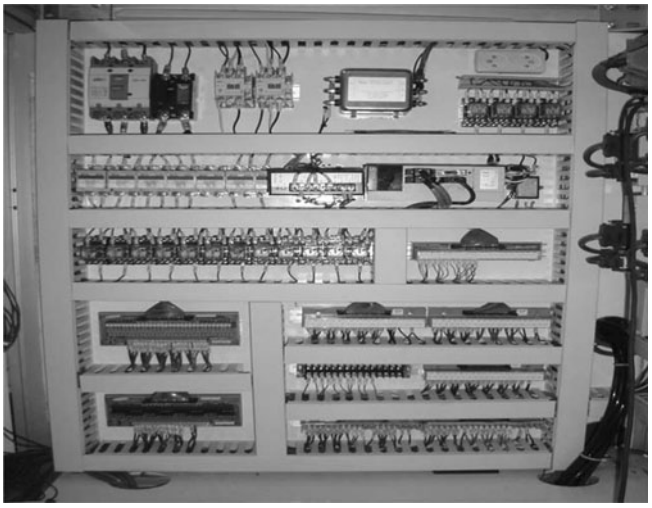


Fig. 7. I/O interface system with PLC.

https://doi.org/10.1017/S026357470700358X Published online by Cambridge University Press

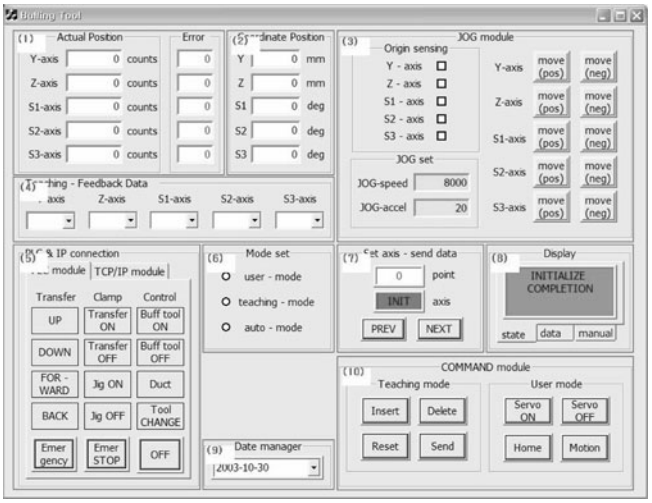


Fig. 8. GUI program for buffing control.

programming language. The header file and library for the control functions are made up of the files provided by the modular multivariable control (MMC) control system, whose architecture is open to the public. Based on visual C/C++, we developed a GUI program for the operator to program the robot motion with ease, as shown in Figs. 8 and 9. Then, the program contains the closed-form solutions for the joint position and velocity of the robot based on the forward and inverse kinematics. In addition, we have composed the necessary functions for controlling the peripheral systems and interfacing with them in the program.

3.3. GUI program

A GUI program was developed so that the operator can interface with the robot system easily, as shown in Fig. 8. In the GUI program, we adapted the header files and C library provided by the Samsung MMC controller. We composed user-friendly functions related with editing and controlling the motion of the robot for easy usage of the robot, and incorporated them into the GUI program. Also, we developed a control and monitoring program for the motion of robot and peripheral systems. This program is capable of notifying the states of the joint motors along the prescribed trajectory and the position errors. Furthermore, it has the teaching mode which allows the coordination of the robot along the predefined trajectory by the teach pendant. We also composed a computer program with the function of data communication among the host computer, the robot, and peripheral systems in addition to the function of monitoring of the pneumatic actuators. The communication system is operated by the developed transmission control protocol/Internet protocol (TCP/IP).

The GUI program is composed of 10 sections as shown in Fig. 8. Section (1) represents the present encoder states of the motors and tracking errors of the motors between the desired and actual trajectories. Section (2) represents the converted joint angles of the robot according to the gear ratio. Section (3) represents the JOG module, which operates each motor of the robot for teaching and can store the taught data. An example of the source code of the class program for the teaching mode using C language is presented in Fig. 8. Also, the editing of the teaching mode is described in Section (4) where the save, insert, and delete functions are used while editing in the command module. Section (5) describes the function of the PLC, which can control the conveyer, transfer device, fixing jig, and other operations in sequence. Section (6) entitled as MODE SET represents the selection of three modes: user, teaching, and auto. The user mode makes it possible to test the motion of the joint motors step by step, and the teaching mode makes JOG operation possible, and, finally, the auto mode

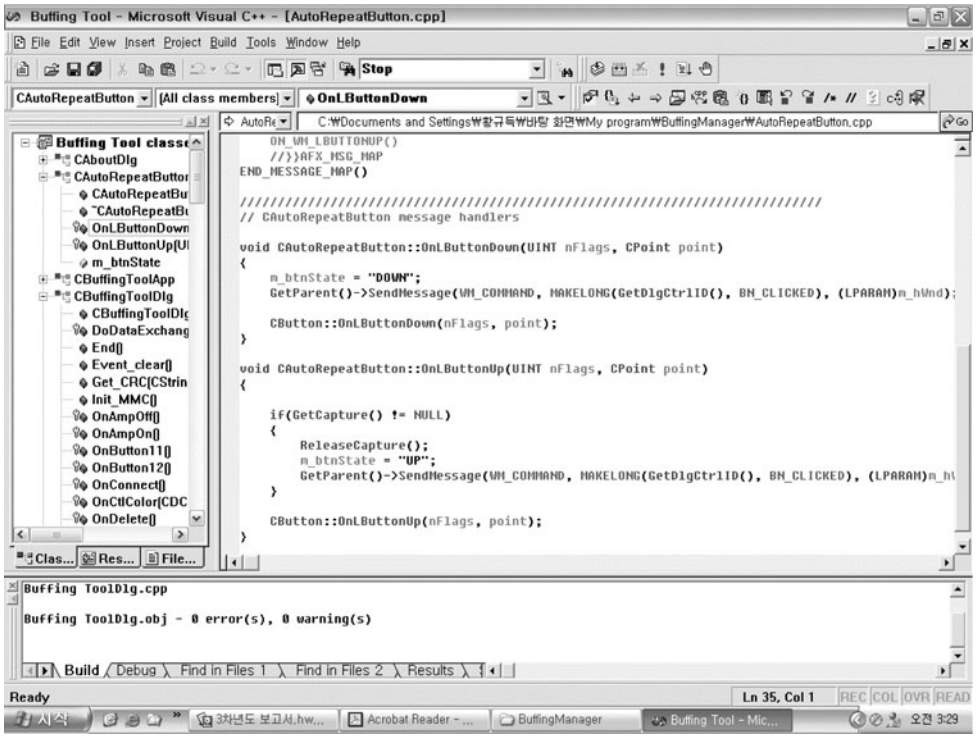


Fig. 9. Code for JOG function library.

https://doi.org/10.1017/S026357470700358X Published online by Cambridge University Press

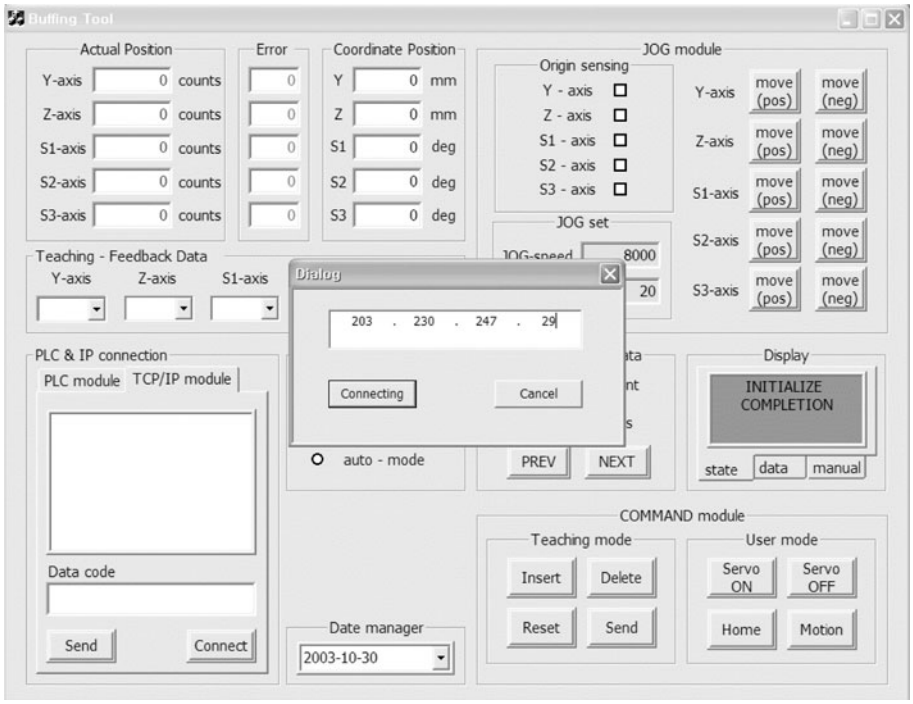


Fig. 10. GUI program with TCP/IP function.

makes it possible to operate the joint motors according to the predefined trajectory data. Section (7) entitled as Set-axis & Send data represents the function of selection of the joint axis sending or inserting teaching data. Section (8) offers the display function composed of the automatic and manual modes. Section (9) represents the function of displaying of the time related with the sequential processes. Section (10) provides the functions of the command modules selecting the teaching mode and serving mode of the joint motors. Moreover, the GUI has a JOG button to teach the manipulator for playback motion, and also has a function to define the desired velocity and acceleration. Fig. 9 shows an example of the display of the source code for the JOG function.

3.4. Communication system

The designed robot system operates in conjunction with the peripheral systems in the sequential mode, but for buffing operations, the controller for the robot was designed to operate in the continuous mode. For sequential operation connecting the robot with the peripheral systems, a TCP/IP protocol was developed as a communication tool.

Using the TCP/IP protocol, the networked control system can transmit the state information of the buffing robot to the server computer which controls all of the shoe production lines. The developed system establishes communication units between the server and client by using the win socket method, and can monitor the motion and state of the system in line in real-time. By hitting the button of "connect" on the GUI program as shown in Fig. 10, the window of the IP address pops up to allow connection with the designated IP address. Also, the module of "Date manager" gives the information of the event time, so that the total time for the production per working day can be measured.

4. Flexible Toolholder

It should be noted that manufactured shoes actually have some differences in size and shape, and even have nonuniform surfaces because of items such as stitched lines. For this reason, some position errors occur in buffing the side of the shoes along the trajectories generated by using model shoes. For automation of the uniform buffing process, the stiff buffing tool at the tip of the robot should have the flexibility to compensate for the regular contact force between the tool and shoes. For this, a new FTH with three directional compliances was developed to compensate for the contact force between the tool and shoes. In this paper, we propose an analysis of the FTH with three directional compliances based on the compressive spring, whose structure is shown in Figs. 11 and 12. The FTH is designed to provide compliance along three directions. It can be observed that the compliant function of the FTH diminishes the position errors occurring in buffing the side of shoes along the trajectories generated using the model shoe such that the FTH makes it possible to yield even buffed surface despite the nonuniform surface of the shoes.

As shown in Fig. 13, the FTH is composed of two parts where the upper part the rotating motor and the lower part the deburring tool. The upper part is made up of two independent

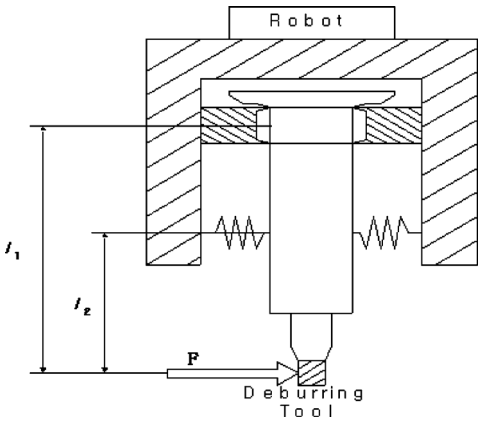


Fig. 11. Structure of toolholder.

https://doi.org/10.1017/S026357470700358X Published online by Cambridge University Press

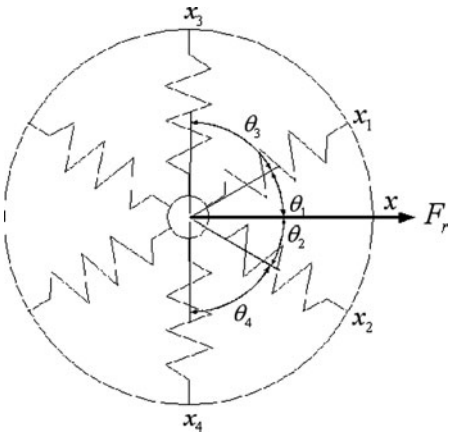


Fig. 12. Cross section of toolholder.

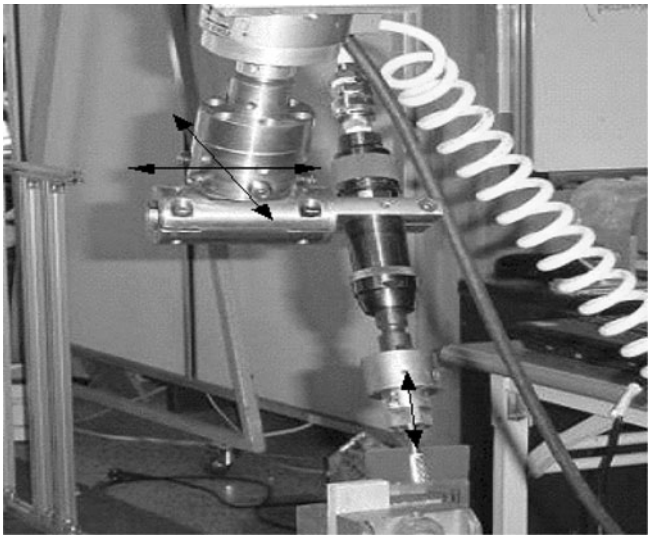


Fig. 13. Compliance direction of flexible toolholder.

compressive springs, which give two-dimensional compliance to the motor holding the rotating deburring tool. The lower part attached to the rotating shaft of the motor has compliance along the axis of the shaft such that it complies according to the excessive applied force between the tool and the shoe.

Here, the force relations of the FTH are analyzed. The related equation between the complied force F_r and the contact force F between the tool and shoe is described as

$$F_r = \frac{l_2}{l_1} F = kx(\cos\theta_1 + \cos\theta_2 + \cos\theta_3 + \cos\theta_4) \quad (14)$$

where k is the spring coefficient. Note that the relative angles of the compressive springs are given as $\theta_2 = 60^\circ - \theta_1$, $\theta_3 = 60^\circ + \theta_1$, and $\theta_4 = 60^\circ + \theta_2 = 120^\circ - \theta_1$ where since the angle between the springs is 60°, the constraint is $0^\circ \leq \theta_1 \leq 60^\circ$. A simplified force analysis on the FTH is included in the Appendix.

5. Buffing Test of Shoes

Using the developed buffing robot with the FTH, a buffing test was performed. The buffing trajectory for the side of the shoe was taught in the JOG mode in Section 9 of the GUI. After teaching the operation, the data of the trajectory for the robot to follow were generated. Using the motion command, a command to follow the taught points was sent to the robot. The test time for buffing the side of the shoe took 16 s, and the side of the shoe was buffed appropriately for gluing. Figs. 14 (a) and (b) show the buffing process of the side of the shoe, and Fig. 15 illustrates the buffed side of the shoe through the buffing test. Note that a buffing test without the FTH yielded irregular buffing surface or sticking of the tool to the side of the shoe.

6. Conclusion

In this paper, we have presented a new practical five-axis robot for buffing public shoes. Based on an analysis on the forward and inverse kinematics for automatic buffing operations, we derived analytic solutions for the joint angles corresponding to the position and orientation of the tool in the Cartesian coordinates. Also, we developed the peripheral systems of the robot for sequential buffing processes, and a TCP/IP protocol for communication between the robot and the peripheral systems. Furthermore, we built GUI programs, including the functions of the robot operations and communication for easy usage of the robot. To compensate for the excessive applied force to deburring tools, a new FTH has been proposed and analyzed.

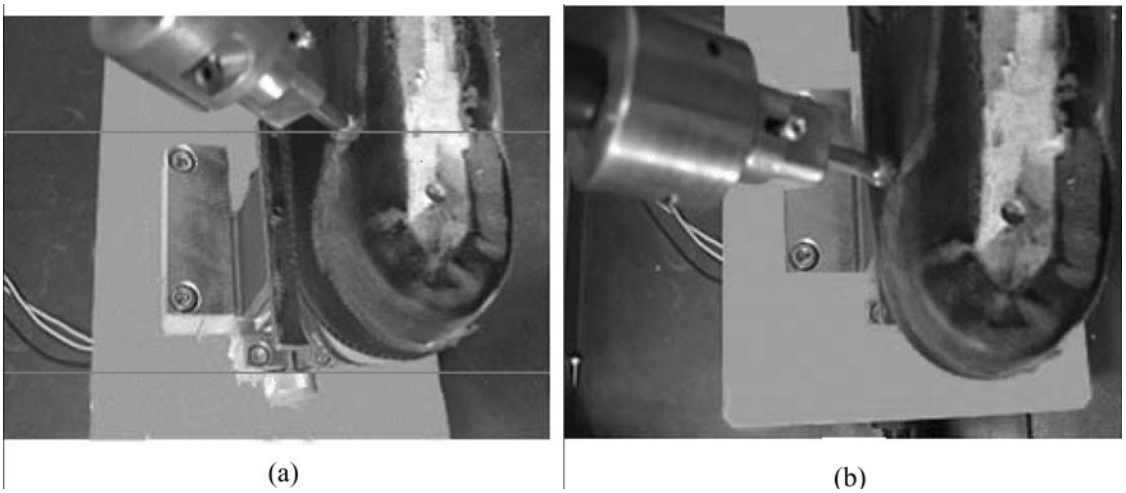


Fig. 14. The buffing process.

https://doi.org/10.1017/S026357470700358X Published online by Cambridge University Press

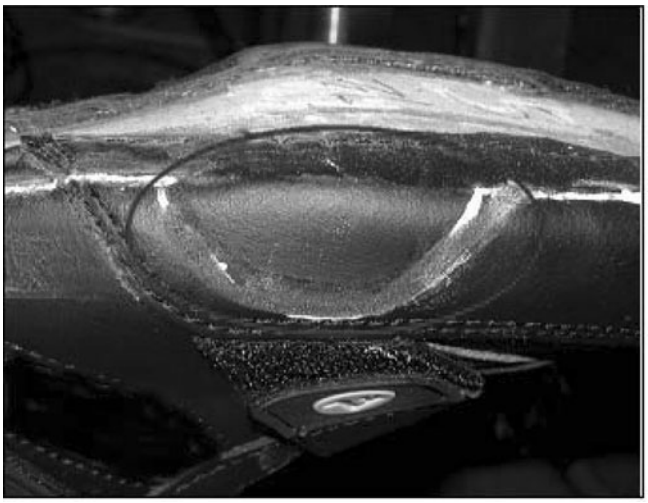


Fig. 15. The buffed shoe.

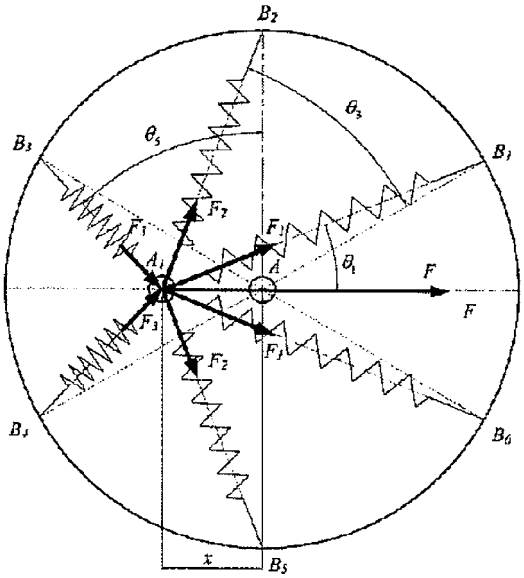


Fig. 16. Cross section of tool holder.

Through the experimental test of the integrated system using the GUI program including the TCP/IP communication system, which notifies the information on the sequential operations of the robot and the peripheral systems, it was shown that the presented scheme offers successful sequential operations. Finally, we confirmed good performance of buffing operations and deburring process with the proposed FTH through a buffing test of the shoes.

Acknowledgment

This study was supported by a Research Grant from the Underwater Vehicle Research Center of Defense Acquisition Program Administration and Agency for Defense Development, Korea. This financial support is gratefully acknowledged.

References

1. J. E. Spencer, "Robotics technology and the advent of agile manufacturing systems in the footwear industry and robot manipulators," *Assem. Autom.* **16**(3), 10–15 (1996).
2. B. W. Rooks, "Robots bring automation to shoe production," *Assem. Autom.* **16**(3), 22–25 (1996).
3. O. Botema and B. Roth, *Theoretical Kinematics* (North Holland, Amsterdam, The Netherland, 1979).
4. J. C. Colson and N. D. Perreira, "Kinematic Arrangements Used in Industrial Robots," *Proceedings of the 13th International Symposium on Industrial Robots*, (1983), pp. 540–544.
5. T. S. Todorov, "Synthesis of four-bar mechanism by Freudenstein–Chebyshev," *Mech. Mach. Theory* **37**, 1505–1512 (June 2002).
6. M. W. Spong and M. Vidyasagar, *Robot Dynamics and Control* (Wiley, Hoboken, NJ, 1989).

Appendix

Simplified force analysis of FTH

The total spring force F is obtained on the basis of the following simplified assumptions: (1) The loads are symmetrical with respect to the x-axis. (2) The springs lie at a plane after deflection. The body of the deburring tool is in equilibrium state in point A. On applying some load at the tool, the point A is moved to point A_1. Because of symmetry at the tool, the forces act as

$$F_1 = k(l_1 + l_0 - l), \tag{A1}$$

$$F_2 = k(l_2 + l_0 - l), \tag{A2}$$

$$F_3 = k(l - l_3 - l_0), \tag{A3}$$

where k is the stiffness of a spring, l is the spring length in the equilibrium state, e.g.,

$$l_1 = A_1B_1 = A_1B_6,$$
$$l_2 = A_1B_2 = A_1B_5,$$
$$l_3 = A_1B_3 = A_1B_4$$

are the lengths of the spring, and the force is

$$F = 2F_{1x} + 2F_{2x} + 2F_{3x} \tag{A4}$$

where

$$F_{1x} = F_1 \cos\theta_1, \tag{A5}$$

$$F_{2x} = F_2 \cos(30^\circ + \theta_3), \tag{A6}$$

$$F_{3x} = F_3 \cos(90^\circ - \theta_5). \tag{A7}$$

The deflected length l_1 can be expressed from the triangle AA_1B_1 as

$$l_1 = \sqrt{x^3 + l^2 + \sqrt{3}xl} \tag{A8}$$

where $x = AA_1$. From the same triangl, it follows that

$$\cos\theta_1 = \frac{2x + \sqrt{3}l}{2l_1}. \tag{A9}$$

By analogy, it works out that

$$l_2 = \sqrt{x^2 + l^2} \tag{A10}$$

$$\cos(30^\circ + \theta_3) = \frac{x}{\sqrt{x^2 + l^2}} \tag{A11}$$

$$l_3 = \sqrt{x^2 + l^2 - \sqrt{3}xl} \tag{A12}$$

$$\cos(90^\circ - \theta_5) = \frac{\sqrt{3}l - 2x}{2l_3}. \tag{A13}$$

https://doi.org/10.1017/S026357470700358X Published online by Cambridge University Press